Solubility of H_2S in Ionic Liquids 1-Ethyl-3-methylimidazolium Hexafluorophosphate ([emim][PF_6]) and 1-Ethyl-3-methylimidazolium Bis(trifluoromethyl)sulfonylimide ([emim][Tf_2N])

Hossein Sakhaeinia,[†] **Amir Hossein Jalili,**[‡] **Vahid Taghikhani,***[,†] **and Ali Akbar Safekordi**[§]

Department of Chemical Engineering, Sciences and Research Branch, Islamic Azad University (IAU), Tehran, Iran, Gas Science Department, Gas Research Division, Research Institute of Petroleum Industry (RIPI), National Iranian Oil Company (NIOC), P.O. Box 14665-137, West Blvd. Azadi Sport Complex, Tehran, Iran, and Department of Chemical and Petroleum Engineering, Sharif University of Technology, Azadi Ave., Tehran, Iran

The solubility of hydrogen sulfide gas in ionic liquids (ILs) 1-ethyl-3-methylimidazolium hexafluorophosphate ([emim][PF_6]) at temperatures from (333.15 to 363.15) K and 1-ethyl-3-methylimidazolium bis(trifluoromethyl)sulfonylimide ([emim][Tf_2N]) at temperatures ranging from (303.15 to 353.15) K and pressures up to about 2.0 MPa was measured using a volumetric based static apparatus. The solubility data were correlated using two models: the Krichevsky−Kasarnovsky (KK) equation, and the extended Henry's law combined with the Pitzer's virial expansion for the excess Gibbs energy. Henry's law constants (at zero pressure) were obtained at different temperatures from the obtained experimental solubility data. Using the solubility data, the partial molar thermodynamic functions of solution, that is, Gibbs energy, enthalpy, and entropy were calculated. A comparison showed that the solubility of H_2S in [emim][Tf_2N] is greater than [emim][PF_6].

Introduction

Hydrogen sulfide is one of the most abundant sulfur-containing compounds in natural gas and light and middle distillate oil fractions. Because of its undesirable high toxicity and corrosiveness, hydrogen sulfide must be removed from industrial gas and oil streams. Currently aqueous solutions of single or binary mixtures of alkanolamines such as monoethanolamine (MEA), diethanolamine (DEA), *N*-methyldiethanolamine (MDEA), and di-isopropanolamine (DIPA) are in use for the removal of H_2S and CO_2 from natural gas as well as refinery and synthesis gas streams in industry.[1] The process involves absorption followed by the chemical reaction of H_2S and CO_2 with the alkanolamine solution in a plate column at low temperatures (at about 315 K) and variable pressures (up to about 7 MPa). There are some disadvantages associated with the commercial use of these alkanolamine solutions, including: (1) loss of alkanolamine and transfer of water into the gas stream during desorption stage,[2] (2) oxidative degradation of alkanolamines to form corrosive byproducts,[2] and (3) a relatively high heat capacity of the solvent water and also a large enthalpy of reaction of the acid gases with alkanolamines, which demand high energy consumption during the desorption stage of the process.[3] These drawbacks have attracted the attention of many active researchers in the field of gas sweetening as well as gas separation areas toward the use of newly emerged chemical compounds known as room temperature ionic liquids (RTILs).[4] RTILs, also known as liquid salts, ionic melts, and liquid electrolytes, are a class of organic compounds comprised of an organic cation like quaternary ammonium, imidazolium, and pyridinium ions and an inorganic or organic anion such as $[Cl]^-$, $[BF_4]^-$, $[PF_6]^-$, or $[Tf_2N]^-$, which are liquid over an extended temperature range including ambience (below boiling point of water).[4] Because of the existence of Coulombic attraction between the ions of RTILs, they have a negligibly small vapor pressure and high thermal and electrochemical stability.[4] These compounds, which were formerly used for specialized electrochemical applications, have attained growing attention since 1995 in diverse practical areas as solvent media for reaction synthesis, supercritical CO_2 extraction, gas separation, and purification.[4] Some people have proposed amine-functionalized task-specific ionic liquids as an alternative to conventional alkanolamine solutions for the removal of acid gases (CO_2 and H_2S) in gas sweetening processes.[5]

Knowledge about the solubility and the rate of solubility, that is, diffusion coefficients of gases at various temperatures and pressures, is an important feature in the evaluation of ionic liquids (ILs) for use in industrial natural gas treating processes. Experimental data for the solubility and diffusion of hydrogen sulfide in ILs are scarce and include the following: (1) The data reported by Jou and Mather[6] for the solubility of H_2S in 1-butyl-3-methylimidazolium hexafluorophosphate ([bmim][PF_6]) at temperatures from (298.15 to 403.15) K and pressures up to 9.6 MPa. They have correlated the experimental solubility data by the Krichevsky−Kasarnovsky (KK) equation to obtain Henry's law constant and thermodynamic properties of solution at the studied temperatures and concluded that the ILs are useful for the bulk removal of the acid gases at high acid gas partial pressures. (2) Those reported by Pomelli et al.[7] for the solubility of H_2S in different $[bmim]^+$-based ILs with different anions and in a series of bis(trifluoromethyl)sulfonylimide ($[Tf_2N]^-$) ILs with different cations at $T = 298.15$ K and $P = 1.4$ MPa. They used a medium-pressure NMR spectroscopic technique to

---

* Corresponding author. E-mail: taghikhani@sharif.edu. Tel.: 98 21-44802841.

[†] Islamic Azad University, Sciences and Research Branch.

[‡] Research Institute of Petroleum Industry (RIPI), National Iranian Oil Company (NIOC).

[§] Sharif University of Technology.

10.1021/je100794k

measure the solubility and observed that H_2S is stable with no sign of reaction under the investigated experimental conditions. Their quantum chemical calculations show that the interaction energy between H_2S and the anion part of the ILs is comparable in strength to traditional hydrogen bonds and concluded that this is the main factor responsible for the high solubility of hydrogen sulfide in ILs. (3) The recently published data of Heintz et al.[8] for the solubility of a mixture of N_2/H_2S in an ammonium-based IL with an approximate chemical formula from (300 to 500) K and pressures up to 0.23 MPa. Their aim was to use ILs for the removal of H_2S and CO_2 acid gases from fuel gas streams and observed that the solubility of H_2S is greater than that of CO_2 in the IL studied and proposed that the ammonium-based IL is an appropriate solvent for the removal of H_2S from syngas streams. (4) The recent vapor−liquid−liquid equilibrium (VLLE) data of Shifflet and Yokozeki[9] for H_2S/[bmim][PF_6] binary mixtures at temperatures ranging from (273 to 342) K and H_2S/CO_2/[bmim][PF_6] ternary mixtures at temperatures of T = (298.15, 323.15, and 348.15) K. They proposed a generic Redlich−Kwong equation of state (RK EoS) to model the obtained experimental data and concluded that the Type V phase behavior predicted by the RK EoS is in good agreement with their VLLE measurements for CO_2/[bmim][PF_6] and H_2S/[bmim][PF_6] systems. (5) Finally, the data produced in our laboratory at temperatures ranging from (303.15 to 353.15) K and pressures up to 1.6 MPa, which include the solubility of H_2S in [bmim]$^+$- and [hmim]$^+$-based ILs with different anions,[10,11] the solubility and diffusion of H_2S and CO_2 in 1-(2-hydroxyethyl)-3-methylimidazolium tetrafluoroborate ([hemim][BF_4])[12] and in 1-ethyl-3-methylimidazolium ethylsulfate ([emim][$EtSO_4$]),[13] and most recently the solubility of H_2S in [hemim][PF_6], [hemim][OTf], and [hemim][Tf_2N].[14] All of the data obtained have been used to estimate Henry's law constants at different temperatures. Overall, it can be concluded from the experimental data produced in our laboratory that the solubility of H_2S in a given IL is greater than that of CO_2 and the solubility of H_2S in ILs follows the same behavior as that of CO_2; namely, their solubilities increase as the number of $-CF_3$ groups in the anion part of ILs with the same cation increases. Also, the effect of the anion on the solubility of H_2S is more pronounced than the cation, and the solubility increases as the alkyl chain length attached to the imidazolium cation increases.

In this work, which is part of an ongoing study on the solubility behavior of H_2S and CO_2 acid gases, in ILs, our first aim is to take a step toward completing a data bank for solubility data and Henry's law constants for H_2S/IL binary mixtures. In this way the equilibrium solubility of H_2S in the ILs [emim][PF_6] at five temperatures from (333.15 to 363.15) K and in [emim][Tf_2N] at six temperatures from (303.15 to 353.15) K at pressures up to 2.0 MPa was measured. The solubilities determined were used to estimate zero pressure Henry's law constants and partial molar thermodynamic functions of solution of H_2S at different temperatures. Correlation equations for the obtained Henry's law constants with temperature are presented here. The results obtained are compared with [emim][$EtSO_4$]-[13] and [hemim]$^+$-based ILs obtained in previous works,[12,14] thus fulfilling our second aim, that is, to investigate the effect of the presence of a hydroxyl group attached to the alkyl chain of cation on the solubility behavior of H_2S in ILs. The obtained solubility data were also correlated by using two models, namely, the KK equation and the extended Henry's law combined with the Pitzer's model for electrolytes (Pitzer's model), the former not taking into account the nonideality of the solute in the liquid phase.

Experimental Section

Materials. Hydrogen sulfide (c.p. grade 99.95 % min) was supplied by Roham Gas Company. The IL [emim][PF_6] (CAS Registry No. 155371-19-0) was obtained from Fluka with nominal purity > 97 %, and [emim][Tf_2N] (CAS Registry No. 174899-82-2) was obtained from Merck with a nominal purity of > 99 %. Both of them were used as purchased without further purification.

Apparatus and Procedure. The experimental method for gas solubility measurement has been presented elsewhere in detail,[10−12] and a short description will be given here. In this technique, known quantities of gaseous solute and degassed solvent are contacted at a constant temperature inside an equilibrium cell of known volume. Once the thermodynamic equilibrium is reached, the pressure above the liquid solution becomes constant and is directly proportional with the solubility of the gas in the liquid. The difference between two *PVT* measurements is then used to calculate the quantity of solute present in the liquid solution, $n^{\mathrm{l}}_{\mathrm{solute}}$: first, on introduction of the gas from a container of known volume into the equilibrium cell containing the IL, and second, after thermodynamic equilibrium is reached (i.e., when autoclave pressure remains constant and no longer changes with time):

$$n^{\mathrm{l}}_{\mathrm{solute}} = n_{\mathrm{total}} - n^{\mathrm{g}}_{\mathrm{solute}} \tag{1}$$

where n_{total} is the total number of H_2S moles injected from the gas container into the autoclave and calculated using the following equation:

$$n_{\mathrm{total}} = \frac{V_{\mathrm{gc}}}{RT_{\mathrm{gc}}}\left(\frac{P_{\mathrm{i}}}{Z_{\mathrm{i}}} - \frac{P_{\mathrm{f}}}{Z_{\mathrm{f}}}\right) \tag{2}$$

where V_{gc} denotes the volume of the gas container, Z_{i} and Z_{f} are the compressibility factors corresponding to the initial and final pressures P_{i} and P_{f}, respectively, in the gas container prior to and following gas transfer, R is the universal gas constant, and T_{gc} is the temperature of the gas container. $n^{\mathrm{g}}_{\mathrm{solute}}$ in eq 1 is the number of moles of gas solute left in the gas phase and was determined from the following equation:

$$n^{\mathrm{g}}_{\mathrm{solute}} = \frac{V_{\mathrm{g}}P}{ZRT} \tag{3}$$

where V_{g} is the volume of the gas-phase above IL phase, T is the equilibrium temperature of the cell, and Z is the compressibility factor of gas solute at P and T. In all experiments, the IL was dried in vacuo (below 1.0 kPa) before solubility measurements for about 48 h at a temperature of 343 K to remove trace amounts of moisture and volatile impurities. In the case of [emim][PF_6], a chloride ion test showed no detectable Cl^- ion to be present in the IL. Using a Mettler model DL-37 Karl Fischer volumetric titrator, the water content of ILs was found to be below 100 ± 10 ppm. The temperature of the double-wall equilibrium cell, which was connected to a water recirculation bath (PMT Tamson model T 2500) with a temperature stability within ± 0.02 K, was measured with a Lutron model

TM-917 digital thermometer with a 0.01 K resolution using a Pt-100 sensor inserted into the cell. The equilibrium cell and the gas container pressures were measured using a Keller model PA-33X pressure transmitter sensors in the range of (0 to 2) MPa and (0 to 3) MPa, respectively, which were uncertain to within 0.01 % of their full scale. The calibration of pressure sensors was carried out against a pneumatic dead-weight gauge (DH Budenberg model 550).

The most accurate *PVT* data presented by National Institute of Standards and Technology (NIST) for pure compounds[15] were used to calculate compressibility factors, which were needed for solubility calculations.

Correlation of Experimental Data. Two correlation methods were applied to the experimental data obtained in this work. The first method used was the KK equation:[16]

$$\ln \frac{f_2(T,P)}{x_2} = \ln K_{\mathrm{h},x}^{(P_1^{\mathrm{s}})}(T) + \frac{V_2^{\infty}(P - P_1^{\mathrm{s}})}{RT} \qquad (4)$$

where $f_2(T,P)$ is the fugacity of hydrogen sulfide in the gas phase at temperature T and pressure P, x_2 is the mole fraction of solute in the solvent 1, $K_{\mathrm{h},x}^{P_1^{\mathrm{s}}}(T)$ is Henry's law constant on mole-fraction scale of gas solute 2 in solvent 1 (at the vapor pressure of the solvent),[17] V_2^{∞} is the partial molar volume of gas solute 2 at infinite dilution, and R is the universal gas constant. In this case the vapor pressure of the solvent, the IL, is negligible, and it is reasonable to assume the saturated vapor pressure P_1^{s} is zero. Therefore, f_2 can be substituted by the fugacity of pure hydrogen sulfide gas, f_2^0. Equation 4 can then be rearranged to obtain eq 5

$$\ln \frac{f_2^0(T,P)}{x_2} = \ln K_{\mathrm{h},x}^{(0)}(T) + \frac{V_2^{\infty}P}{RT} \qquad (5)$$

Values of $K_{\mathrm{h},x}^{(0)}(T)$ and V_2^{∞} at each temperature T can be obtained from the intercept and slope of plots of $\ln(f_2^0/x_2)$ versus P at the specified temperature, respectively.

The second method used was the extended Henry's law, which takes into account the nonideality of the solute, H_2S, in the liquid IL phase (Pitzer's model)

$$K_{\mathrm{h},m}(T,P)a_m(T,m_2) = f_2(T,P) \qquad (6)$$

$K_{\mathrm{h},m}(T,P)$ is the molality-scale Henry's constant of the solute (H_2S) in the IL at temperature T and pressure P. $a_m(T,m_2)$ is the activity of the gas solute in the liquid phase (IL), which is related to the molality m_2 of the gas solute and activity coefficient γ_2 through eq 7:

$$a_m(T,m_2) = \frac{m_2}{m^{\mathrm{o}}}\gamma_2 \qquad (7)$$

where $m^{\mathrm{o}} = 1\ \mathrm{mol \cdot kg^{-1}}$. The relation between $K_{\mathrm{h,m}}(T,P)$ and Henry's law constant at zero pressure, $K_{\mathrm{h,m}}^{(0)}(T)$, is expressed as[17]

$$K_{\mathrm{h,m}}(T,P) = K_{\mathrm{h,m}}^{(0)}(T)\exp\left(\frac{V_2^{\infty}P}{RT}\right) \qquad (8)$$

The activity coefficient of solute, γ_2, in the IL was calculated using the Pitzer's virial expansion for the excess Gibbs free energy (molality-scale):[18,19]

$$\ln \gamma_2 = 2 \cdot \frac{m_2}{m^{\mathrm{o}}} \cdot \beta_2 + 3\left(\frac{m_2}{m^{\mathrm{o}}}\right)^2 \cdot \beta_3 \qquad (9)$$

Here β_2 and β_3 are the dimensionless parameters describing binary and ternary interactions between gas molecules in the solvent, respectively.

The fugacity of pure gas (hydrogen sulfide), $f_2^0(T,P)$, is the product of the total pressure P and fugacity coefficient $\phi(T,P)$

$$f_2^0(T,P) = \phi(T,P)P \qquad (10)$$

In both of the above-mentioned models, the fugacity coefficient was calculated using the most accurate corresponding states developed by NIST for pure compounds.[15] This way the numerical values of the molar volume of H_2S as a function of pressure at each isotherm (reported by NIST) were first fitted with a fifth-order Padé approximant[20] with 11 adjustable parameters. This function can empirically describe the volumetric $P-V$ behavior of H_2S with a good degree of accuracy. In the next step, the fugacity coefficient can be calculated using the fundamental equation for the fugacity coefficient of pure fluids,[17] that is,

$$\ln \phi = \int_0^P (P\bar{V}/RT - 1)\, \mathrm{d}P/P$$

followed by a simple numerical integration. The fugacities estimated in this way for H_2S agreed within 1 % with those calculated by using the Peng−Robinson EoS[21] in the pressure range studied in this work.

The Henry's law constant on the molality scale, $K_{\mathrm{h},m}^{(0)}(T)$, is related to Henry's law constant on the mole fraction scale, $K_{\mathrm{h},x}^{(0)}(T)$, by

$$K_{\mathrm{h},m}^{(0)}(T) = K_{\mathrm{h},x}^{(0)}(T) \cdot \frac{M_{\mathrm{solv}}}{1000} \qquad (11)$$

where M_{solv} is the molar mass of the solvent in $\mathrm{g \cdot mol^{-1}}$.

Results and Discussion

The results of solubility measurement of hydrogen sulfide in the ILs [emim][PF_6] and [emim][Tf_2N] are summarized in Tables 1 and 2 along with their corresponding standard deviations and are graphically shown in Figures 1 and 2, respectively. The reliability and accuracy of the method of measurement have been checked in our previous works.[10,13] The measurement temperature starts at 333.15 K, which is about the melting point of [emim][PF_6] claimed by the supplier (Fluka) and also reported by other researchers.[22] However, in the case of [emim][Tf_2N], the measurement temperature starts at 303.15 K. Values of $\ln K_{\mathrm{h},x}^{(0)}$ at each temperature T were obtained from the intercept of the plots of $\ln(f_2^0/x_2)$ versus P at the specified temperature. The corresponding mole fraction-scale Henry's law constants at zero pressure $K_{\mathrm{h},x}^{(0)}$ are listed in Table 3 for the solubility of H_2S in the ILs studied in this work along with their standard

Table 1. Mole Fraction Solubility of Hydrogen Sulfide Gas, x_2, in [emim][PF$_6$]

p/MPa	x_2	p/MPa	x_2	p/MPa	x_2
T/K = 333.15		T/K = 338.15		T/K = 343.15	
0.1449	0.038 ± 0.001	0.1499	0.037 ± 0.001	0.1541	0.036 ± 0.001
0.2970	0.077 ± 0.001	0.3073	0.075 ± 0.001	0.3169	0.072 ± 0.001
0.4830	0.124 ± 0.002	0.5001	0.119 ± 0.001	0.5160	0.116 ± 0.001
0.6852	0.172 ± 0.002	0.7107	0.166 ± 0.002	0.7320	0.161 ± 0.002
0.9227	0.224 ± 0.003	0.9566	0.218 ± 0.003	0.9901	0.212 ± 0.003
1.107	0.265 ± 0.003	1.149	0.257 ± 0.003	1.189	0.249 ± 0.003
1.369	0.318 ± 0.004	1.423	0.308 ± 0.004	1.474	0.300 ± 0.004
1.580	0.359 ± 0.005	1.644	0.348 ± 0.004	1.705	0.339 ± 0.004
T/K = 353.15		T/K = 363.15			
0.1625	0.033 ± 0.001	0.1725	0.032 ± 0.001		
0.3356	0.068 ± 0.001	0.3536	0.064 ± 0.001		
0.5462	0.109 ± 0.001	0.5770	0.102 ± 0.002		
0.7782	0.152 ± 0.002	0.8222	0.143 ± 0.002		
1.052	0.200 ± 0.002	1.112	0.187 ± 0.003		
1.265	0.236 ± 0.003	1.337	0.223 ± 0.003		
1.567	0.285 ± 0.003	1.664	0.270 ± 0.004		
1.822	0.322 ± 0.004	1.933	0.306 ± 0.005		

Table 2. Mole Fraction Solubility of Hydrogen Sulfide Gas, x_2, in [emim][Tf$_2$N]

p/MPa	x_2	p/MPa	x_2	p/MPa	x_2
T/K = 303.15		T/K = 313.15		T/K = 323.15	
0.1077	0.070 ± 0.001	0.1186	0.065 ± 0.001	0.1290	0.059 ± 0.001
0.2145	0.136 ± 0.002	0.2365	0.126 ± 0.001	0.2573	0.118 ± 0.002
0.3629	0.221 ± 0.003	0.4017	0.205 ± 0.002	0.4378	0.190 ± 0.003
0.5816	0.330 ± 0.004	0.6445	0.309 ± 0.004	0.7063	0.291 ± 0.005
0.8115	0.427 ± 0.005	0.9078	0.407 ± 0.005	0.9998	0.387 ± 0.007
1.025	0.506 ± 0.006	1.152	0.481 ± 0.006	1.274	0.465 ± 0.008
1.244	0.567 ± 0.006	1.395	0.541 ± 0.006	1.523	0.523 ± 0.009
1.444	0.609 ± 0.007	1.628	0.584 ± 0.007		
T/K = 333.15		T/K = 343.15		T/K = 353.15	
0.1389	0.056 ± 0.001	0.1483	0.052 ± 0.001	0.1569	0.049 ± 0.001
0.2773	0.108 ± 0.002	0.2963	0.101 ± 0.002	0.3141	0.095 ± 0.002
0.4730	0.178 ± 0.003	0.5060	0.167 ± 0.004	0.5375	0.158 ± 0.004
0.7659	0.273 ± 0.005	0.8214	0.258 ± 0.006	0.8745	0.243 ± 0.006
1.087	0.363 ± 0.006	1.169	0.345 ± 0.008	1.248	0.328 ± 0.007
1.391	0.438 ± 0.008	1.499	0.416 ± 0.009	1.606	0.398 ± 0.009
1.686	0.496 ± 0.009				

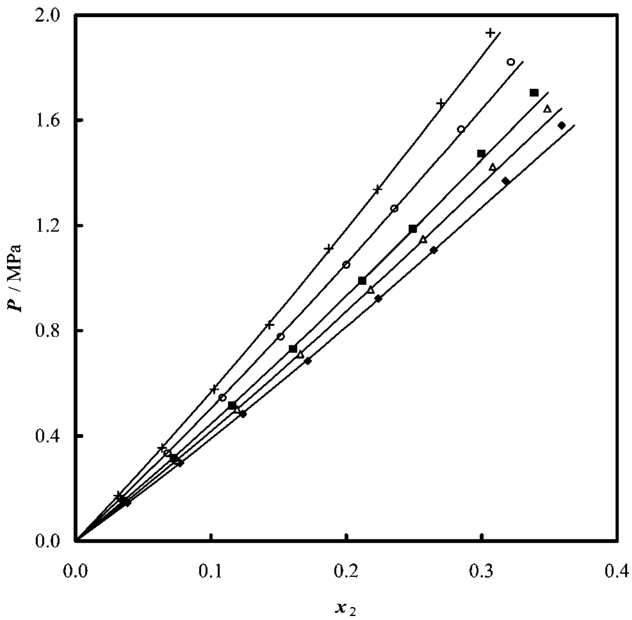

Figure 1. Total pressure above solutions of H_2S + [emim][PF$_6$]: ◆, 333.15 K; △, 338.15 K; ■, 343.15 K; ○, 353.15 K; +, 363.15 K; —, correlation by Pitzer's model.

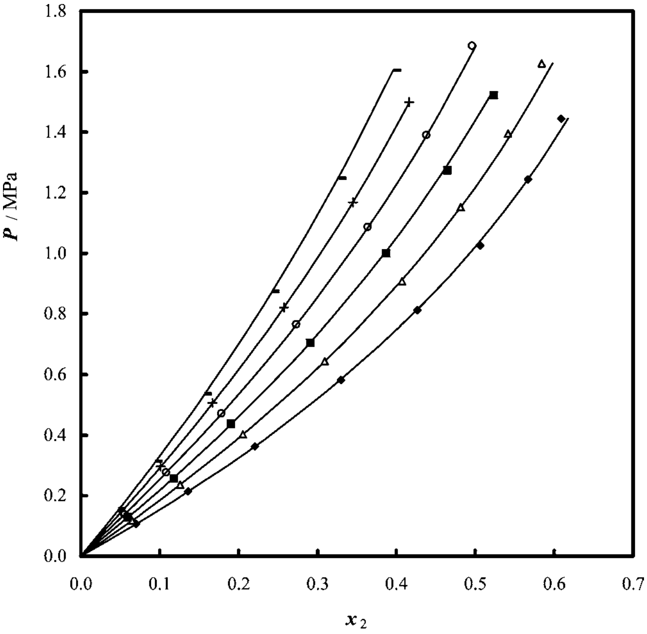

Figure 2. Total pressure above solutions of H_2S + [emim][Tf$_2$N]: ◆, 303.15 K; △, 313.15 K; ■, 323.15 K; ○, 333.15 K; +, 343.15 K; -, 353.15 K; —, correlation by Pitzer's model.

deviations. The $K_{\mathrm{h},x}^{(0)}$ values obtained showed a good correlation with temperature (eq 12).

$$\ln(K_{\mathrm{h},m}^{(0)}/\mathrm{MPa}) = \sum_{i=-1}^{1} A_i (T/\mathrm{K})^i \qquad (12)$$

The obtained parameters A_i of eq 12 are summarized in Table 4. The deviation between experimental and correlated Henry's law constants by means of eq 12 is within experimental uncertainties for $K_{\mathrm{h},x}^{(0)}$ given in Table 3. The Henry's law constants are compared with each other in Figure 3 as a function of temperature. It can be observed that the solubility of hydrogen sulfide in the ILs decreases by increasing the temperature. The curves also indicate that the solubility of H_2S in the ILs studied in this work is typical of that of physical solvents,[10] therefore obeying the Henry's law. It can be observed that the solubility of H_2S in [emim][Tf$_2$N] is about twice that of [emim][PF$_6$]. Also shown in Figure 3 is the variation of the Henry's law constants with temperature for [emim][EtSO$_4$],[13] [hemim][BF$_4$],[12] [hemim][PF$_6$],[14] and [hemim][Tf$_2$N][14] studied in previous works. It can be seen that the solubility of H_2S in [emim]$^+$-based ILs is greater than or comparable to that of [hemim]s with the same anion. Also, the solubility of H_2S in [emim][EtSO$_4$] is the lowest among the [emim]$^+$- and [hemim]$^+$-based ILs studied until now. Comparison reveals that (see Figure 3) increasing the alkyl chain length of the cation results in an increase in the solubility of H_2S in the ILs containing the same anion; thus, the solubility of H_2S in [bmim][PF$_6$] and [bmim][Tf$_2$N], which was studied in previous work,[10] is slightly but not much greater than that of [emim][PF$_6$] and [emim][Tf$_2$N], respectively.

Consideration of the density of pure ILs may provide some useful clues to explain the observed trend in solubility. Plots of molar densities of [emim]s as well as those of [hemim]s against temperature are presented in Figure 4. The molar density of [emim][Tf$_2$N][23] is much lower than that of [emim][PF$_6$];[24] thus, as long as the cations are the same, there is more free volume available in the former case (due to larger size of the anion

Table 3. Thermodynamic Properties of H_2S in [emim][PF_6] and [emim][Tf_2N]

T / K	$K^{(0)}_{h,x}$ / MPa	$\Delta_{sol}G^{\infty}_{x}$ / $kJ \cdot mol^{-1}$	$\Delta_{sol}H^{\infty}_{x}$ / $kJ \cdot mol^{-1}$	$\Delta_{sol}S^{\infty}_{x}$ / $J \cdot mol^{-1} \cdot K^{-1}$
		[emim][PF_6]		
333.15	3.74 ± 0.03	10.0	−11.9	−65.9
338.15	3.99 ± 0.03	10.4	−11.8	−65.6
343.15	4.24 ± 0.03	10.7	−11.7	−65.2
353.15	4.76 ± 0.03	11.3	−11.5	−64.6
363.15	5.29 ± 0.04	12.0	−11.2	−63.9
		[emim][Tf_2N]		
303.15	1.48 ± 0.01	6.79	−15.0	−71.8
313.15	1.78 ± 0.01	7.50	−14.4	−69.8
323.15	2.11 ± 0.01	8.19	−13.7	−67.9
333.15	2.45 ± 0.01	8.86	−13.1	−65.9
343.15	2.80 ± 0.01	9.51	−12.4	−63.9
353.15	3.16 ± 0.01	10.1	−11.7	−62.0

Table 4. Numerical Values of the Parameters of Equations 12, 13, and 14

A_{-1}	A_0	A_1	B_0	B_1	C_0	C_1
			[emim][PF_6]			
−1872.05	6.5539	−0.00297	4.3408	−0.00879	−0.11904	10.278
			[emim][Tf_2N]			
−2871.63	12.4535	−0.01165	−4395.04	10.169	0.13913	−36.869

[Tf_2N]$^-$ with respect to [PF_6]$^-$) to accommodate H_2S molecules, which results in the higher solubility of H_2S in [emim][Tf_2N] than in [emim][PF_6]. It must be emphasized that the density of [emim][PF_6] is estimated from the predictive method developed by Ye and Shreeve,[24] and therefore some systematic error may be present in the estimated values. This same relation between density and solubility can also be observed in the case of [hemim][Tf_2N] and [hemim][PF_6]. Comparing the densities of [emim][Tf_2N] and [hemim][Tf_2N], one can conclude in a similar way that the solubility of H_2S in [emim][Tf_2N] is higher than or comparable to that of [hemim][Tf_2N]. The difference in density can be ascribed to higher cation size in [hemim][Tf_2N], which results from the presence of an additional hydroxyl −OH group attached to the ethyl substituent in the imidazolium ring. In the case of [emim][PF_6] and [hemim][PF_6] we can see that they have comparable densities (within experimental and computational errors), the solubility of H_2S in [emim][PF_6] is higher or comparable to that of [hemim][PF_6], and the solubilities correlate relatively well with densities. However, Figure 4 shows that even though the density of [emim][$EtSO_4$] is higher than that of [emim][Tf_2N] and [hemim][Tf_2N] and lower than the other ILs, the solubility of H_2S is the lowest in [emim][$EtSO_4$] among the [emim]- and [hemim]-based ILs considered. This observation reveals that the density or entropic considerations alone are not adequate for complete explanation of the solubility behavior and when the anion does not contain fluorine atoms or $-CF_3$ substituents, energetic parameters must also be taken into account. From the above-mentioned explanations, it can also be inferred that the anion plays the most important role in the solubility behavior of H_2S in ILs. This same conclusion has also been made by Brennecke et al.[25−27] and Jalili et al.,[28] which resulted from their experimental study on the solubility behavior of CO_2 in classical imidazolium-based and [hemim]-based ILs, respectively.

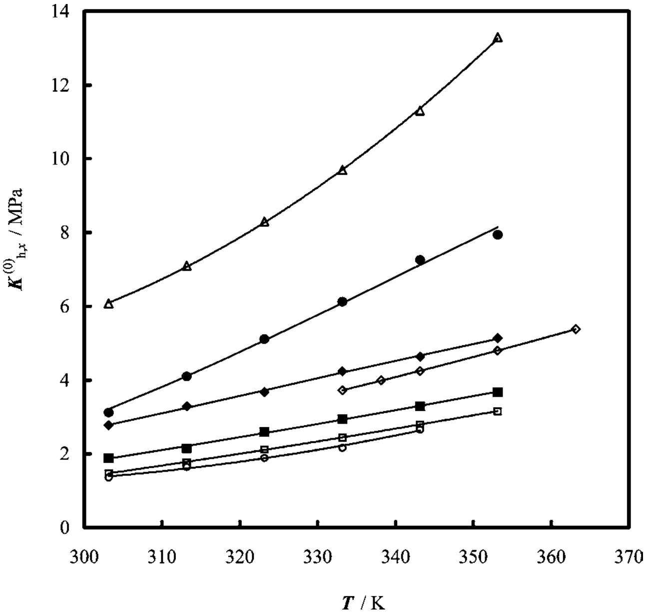

Figure 3. Comparison between Henry's law constants as a function of temperature for the solubility of H_2S in ILs: ◆, [hemim][PF_6] (ref 14); ■, [hemim][Tf_2N] (ref 14); ●, [hemim][BF_4] (ref 12); ◇, [emim][PF_6] (this work); □, [emim][Tf_2N] (this work); △, [emim][$EtSO_4$] (ref 13); ○, [bmim][Tf_2N] (ref 10).

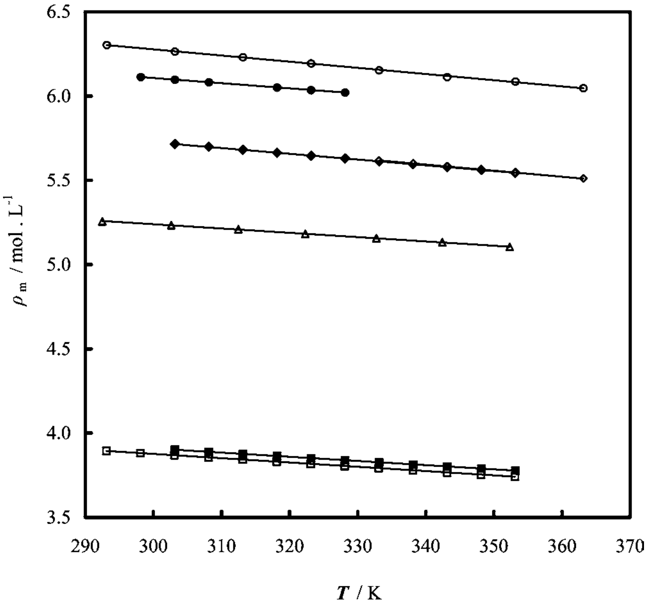

Figure 4. Comparison between molar densities as a function temperature for ILs: ◆, [hemim][PF_6] (ref 14); ■, [hemim][Tf_2N] (ref 14); ●, [hemim][BF_4] (ref 12); ◇, [emim][PF_6] (ref 22); □, [emim][Tf_2N] (ref 21); △, [emim][$EtSO_4$] (ref 13); ○, [emim][BF_4] (ref 31).

As mentioned in previous section, the obtained solubility data were also correlated by using the Pitzer's model. The partial molar volume of gas solute 2 at infinite dilution, V_2^{∞}, was considered a linear function of absolute temperature T defined by eq 13

$$V_2^{\infty}/cm^3 \cdot mol^{-1} = B_0 + B_1(T/K) \qquad (13)$$

where V_2^{∞} is in $cm^3 \cdot mol^{-1}$ and T is in K. The obtained parameters B_0 and B_1 of eq 13 are tabulated in Table 4. Parameter β_2 was considered as a function of temperature T, defined by eq 14, and the ternary interaction parameter β_3 was neglected as far as the systems considered in this work were studied in the medium pressure range (up to 2.0 MPa).

$$\beta_2(T) = C_0 + \frac{C_1}{T/\mathrm{K}} \tag{14}$$

The fitted parameters C_0 and C_1 of eq 14 are presented in Table 4 for each of the systems studied.

The correlations made by the Pitzer's model for the mole fraction of gas solute, H_2S, dissolved in the solvent IL at the specified temperature and pressure, are shown in Figures 1 and 2 for the two systems investigated in this study. It can be seen that there is quite good agreement between the Pitzer's correlation and the obtained experimental data of Tables 1 and 2. The average of relative deviations, ARD, defined by eq 15, and the maximum deviations of correlated mole fractions by using the Pitzer's model, $x_{2,i}^{\mathrm{model}}$, from experimental data, $x_{2,i}$, are summarized in Table 5 for a number of N data points and compared with those correlated by using the KK equation.

$$\mathrm{ARD} = \frac{1}{N}\sum_{i=1}^{N}\left|\frac{x_{2,i}^{\mathrm{model}} - x_{2,i}}{x_{2,i}}\right| \tag{15}$$

Table 5 shows that the Pitzer's model can correlate the experimental solubility data of H_2S in the ILs with higher accuracy than the KK equation except for [emim][PF_6] in which both of them have comparable correlating accuracy. In the case of [emim][PF_6], the solubility of H_2S is the lowest compared to the other IL, and thus, the nonideality in the liquid phase is the lowest. Hence, the KK approach seems to be able to adequately describe the observed solubility behavior.

It can be shown that the Gibbs energy of solution, corresponding to the change in Gibbs energy when the solute is transferred at a constant temperature from the pure perfect gas at the standard pressure to the standard state of infinite dilution of the solute in the solvent, is given by[29]

$$\Delta_{\mathrm{sol}}G_x^{\infty} = RT\ln\left(\frac{K_{\mathrm{h},x}^{(0)}}{P^0}\right) \tag{16}$$

where P^0 is the standard state pressure. The partial molar differences in enthalpy and entropy between the two states can be obtained by calculating the corresponding partial derivatives of the Gibbs energy with respect to temperature

$$\Delta_{\mathrm{sol}}H_x^{\infty} = -T^2\frac{\partial}{\partial T}\left(\frac{\Delta_{\mathrm{sol}}G_x^{\infty}}{T}\right) = -RT^2\frac{\partial}{\partial T}\left[\ln\left(\frac{K_{\mathrm{h},x}^{(0)}}{P^0}\right)\right] \tag{17}$$

$$\Delta_{\mathrm{sol}}S_x^{\infty} = \frac{(\Delta_{\mathrm{sol}}H_x^{\infty} - \Delta_{\mathrm{sol}}G_x^{\infty})}{T} \tag{18}$$

The pressure range considered in this work is not high enough to cause Henry's law constant to be a strong function of pressure, and Henry's law is weakly dependent on pressure under the specified conditions.[10,11] Therefore, it does not give rise to large errors if one ignores this pressure dependency. By means of this approximation and using eqs 16, 17, and 18, we estimated the mole-fraction scale thermodynamic functions of solution at infinite dilution for H_2S in the IL. It may be worth mentioning that the relation between mole fraction scale and molality scale thermodynamic functions of solution is straightforward, and they can be transformed to each other by using eqs 19 and 20,[30]

Table 5. Comparison between Average of Relative Deviations (100 ARD) and Maximum Relative Deviations (100 MRD) of the Calculated from Experimental Mole Fractions by the Two Models Considered in This Work

	Pitzer's model		KK equation	
IL	100 ARD	100 MRD	100 ARD	100 MRD
[emim][PF_6]	0.78	3.0	0.80	3.0
[emim][Tf_2N]	0.49	2.3	1.1	5.2

$$\Delta_{\mathrm{sol}}G_{\mathrm{m}}^{\infty} = \Delta_{\mathrm{sol}}G_x^{\infty} + RT\ln(M_{\mathrm{solu}}/1000) \tag{19}$$

$$\Delta_{\mathrm{sol}}S_{\mathrm{m}}^{\infty} = \Delta_{\mathrm{sol}}S_x^{\infty} - R\ln(M_{\mathrm{solv}}/1000) \tag{20}$$

The values for the mole fraction scale Gibbs energy, $\Delta_{\mathrm{sol}}G_x^{\infty}$, enthalpy, $\Delta_{\mathrm{sol}}H_x^{\infty}$, and entropy $\Delta_{\mathrm{sol}}S_x^{\infty}$, of solution are given in Table 3 at temperatures between (333.15 and 363.15) K and (303.15 to 353.15) K for [emim][PF_6] and [emim][Tf_2N], respectively. As it can be observed, the $\Delta_{\mathrm{sol}}G_x^{\infty}$ values are positive and increase with temperature in a similar manner for the solubility of H_2S in ILs, being the highest for H_2S/[emim][PF_6] and the lowest for H_2S/[emim][Tf_2N]. The $\Delta_{\mathrm{sol}}H_x^{\infty}$ values and $\Delta_{\mathrm{sol}}S_x^{\infty}$ values are negative. The variation with temperature of the $\Delta_{\mathrm{sol}}H_x^{\infty}$ values and $\Delta_{\mathrm{sol}}S_x^{\infty}$ values are positive for H_2S/[emim][PF_6] and H_2S/[emim][Tf_2N], and they increase with temperature. A comparison of $\Delta_{\mathrm{sol}}H_x^{\infty}$ values in Table 3 also reveals that the solubility of H_2S is more favorable in [emim][Tf_2N] than in [emim][PF_6] from an energetic point of view. This is obvious from the difference between enthalpies of solution for the two H_2S/IL systems, which is about 1200 $\mathrm{J \cdot mol^{-1}}$ at 333.15 K and decreases to 200 $\mathrm{J \cdot mol^{-1}}$ at 353.15 K. As long as the cations of the two ILs are the same, the difference in $\Delta_{\mathrm{sol}}H_x^{\infty}$ shows that the interaction energy between H_2S and $[Tf_2N]^-$ is stronger than that of H_2S and $[PF_6]^-$. This conclusion has previously been made by Pomelli et al.[7] by performing quantum chemical calculations. It can be inferred by comparing $\Delta_{\mathrm{sol}}S_x^{\infty}$ values for the two H_2S/IL pairs that the solubility of H_2S is a bit more favorable in [emim][PF_6] than in [emim][Tf_2N] from an entropic point of view. This observation can be explained on the basis of the fact that the interaction energy between $[\mathrm{emim}]^+$ cation and $[PF_6]^-$ anion is stronger than that of $[\mathrm{emim}]^+$ and $[Tf_2N]^-$ (the melting point of [emim][PF_6] is much greater than that of [emim][Tf_2N]). Thus, there exists a more ordered structure in [emim][PF_6] than in [emim][Tf_2N], which gives rise to the observed trend in $\Delta_{\mathrm{sol}}S_x^{\infty}$ values.

Conclusion

New experimental data for the solubility and thermodynamic functions of solution of hydrogen sulfide gas in ILs 1-ethyl-3-imidazolium containing anions hexafluorophosphate and bis(trifluoromethylsulfonyl)imide not previously reported in the literature have been measured and presented in this work. The solubility of H_2S is the highest in [emim][Tf_2N] and the lowest in [emim][PF_6]. The solubility of H_2S in the ILs studied in this work is of a physical nature. The solubility of hydrogen sulfide in [emim]-based ILs is greater than or comparable to [hemim]-based ILs with the same anion. The solubility data can best be correlated by means of an equation composed of the extended Henry's law and Pitzer's virial expansion for the excess Gibbs free energy, that is, by a model, which takes into account the nonideality of solute in the liquid phase. It has been shown that the anion compartment has more profound effect on the solubility behavior of H_2S than the cation in imidazolium-based ILs.

Literature Cited

(1) Kohl, A. L.; Nielsen, R. B. *Gas Purification*, 5th ed.; Gulf Publishing Company: Houston, TX, 1997.

(2) Galán Sánchez, L. M.; Meindersma, G. W.; de Haan, A. B. Solvent Properties of Functionalized Ionic Liquids for CO_2 Absorption. *Chem. Eng. Res. Des.* **2007**, *85*, 31–39.

(3) Camper, D.; Bara, J. E.; Gin, D. L.; Noble, R. D. Room-Temperature Ionic Liquid-Amine Solutions: Tunable Solvents for Efficient and Reversible Capture of CO_2. *Ind. Eng. Chem. Res.* **2008**, *47*, 8496–8498.

(4) Wilkes, J. S. In *Ionic Liquids in Synthesis*; Wasserscheid, P., Welton, T., Eds.; Wiley VCH: Verlag, 2002.

(5) Bates, E. D.; Mayton, R. D.; Ntai, I.; Davis, J. H. CO_2 Capture by a Task-Specific Ionic Liquids. *J. Am. Chem. Soc.* **2002**, *124*, 926–927.

(6) Jou, F.-Y.; Mather, A. E. Solubility of Hydrogen Sulfide in [bmim][PF_6]. *Int. J. Thermophys.* **2007**, *28*, 490–495.

(7) Pomelli, C. S.; Chiappe, C.; Vidis, A.; Laurenczy, G.; Dyson, P. J. Influence of the Interaction Between Hydrogen Sulfide and Ionic Liquids on Solubility: Experimental and Theoretical Investigation. *J. Phys. Chem. B* **2007**, *111*, 13014–13019.

(8) Heintz, Y. J.; Sehabiague, L.; Morsi, B. I.; Jones, K. L.; Luebke, D. R.; Pennline, H. W. Hydrogen Sulfide and Carbon Dioxide Removal from Dry Fuel Gas Streams Using an Ionic Liquid as a Physical Solvent. *Energy Fuels* **2009**, *23*, 4822–4830.

(9) Shiflett, M. B.; Yokozeki, A. Separation of CO_2 and H_2S using room-temperature ionic liquid [bmim][PF_6]. *Fluid Phase Equilib.* **2010**, *294*, 105–113.

(10) Jalili, A. H.; Rahmati-Rostami, M.; Ghotbi, C.; Hosseini-Jenab, M.; Ahmadi, A. N. Solubility of H_2S in Ionic Liquids [bmim][PF_6], [bmim][BF_4] and [bmim][Tf_2N]. *J. Chem. Eng. Data* **2009**, *54*, 1844–1849.

(11) Rahmati-Rostami, M.; Ghotbi, C.; Hosseini-Jenab, M.; Ahmadi, A. N.; Jalili, A. H. Solubility of H_2S in Ionic Liquids [hmim][PF_6], [hmim][BF_4] and [hmim][Tf_2N]. *J. Chem. Thermodyn.* **2009**, *41*, 1052–1055.

(12) Shokouhi, M.; Adibi, M.; Jalili, A. H.; Hosseini-Jenab, M.; Mehdizadeh, A. Solubility and Diffusion of H_2S and CO_2 in the Ionic Liquid 1-(2-Hydroxyethyl)-3-methylimidazolium Tetrafluoroborate. *J. Chem. Eng. Data* **2010**, *55*, 1663–1668.

(13) Jalili, A. H.; Mehdizadeh, A.; Shokouhi, M.; Ahmadi, A. N.; Hosseini-Jenab, M.; Fateminassab, F. Solubility and Diffusion of CO_2 and H_2S in the Ionic Liquid 1-ethyl-3-methylimidazolium ethylsulfate. *J. Chem. Thermodyn.* **2010**, *42*, 1298–1303.

(14) Sakhaeinia, H.; Taghikhani, V.; Jalili, A. H.; Mehdizadeh, A.; Safekordi, A. A. Solubility of H_2S in 1-(2-Hydroxyethyl)-3-methylimidazolium Ionic Liquids with Different Anions. *Fluid Phase Equilib.* **2010**, *298*, 303–309.

(15) NIST Scientific and Technical Databases, Thermophysical Properties of Fluid Systems. http://webbook.nist.gov/chemistry/fluid/ (accessed May 2010).

(16) Krichevsky, I. R.; Kasarnovsky, J. S. Thermodynamical Calculations of Solubilities of Nitrogen and Hydrogen in Water at High Pressures. *J. Am. Chem. Soc.* **1935**, *57*, 2168–2171.

(17) Prausnitz, J. M.; Lichtenthaler, R. N.; Azevedo, E. G. *Molecular Thermodynamics of Fluid Phase Equilibria*, 3rd ed.; Prentice Hall: Englewood Cliffs, NJ, 1999.

(18) Pitzer, K. S. Thermodynamics of Electrolytes. I. Theoretical Basis and General Equations. *J. Phys. Chem.* **1973**, *77*, 268–277.

(19) *Activity Coefficients in Electrolyte Solutions*; Pitzer, K. S., Ed.; CRC Press: Boca Raton, FL, 1991.

(20) Press, W. H.; Flannery, B. P.; Teukolsky, S. A.; Vetterling, W. T. *Numerical Recipes in FORTRAN: The Art of Scientific Computing*, 2nd ed.; Cambridge University Press: Cambridge, 1992.

(21) Peng, D.-Y.; Robinson, D. B. A New Two-Constant Equation of State. *Ind. Eng. Chem. Fundam.* **1976**, *15*, 59–64.

(22) Wong, D. S. H.; Chen, J. P.; Chang, J. M.; Chou, C. H. Phase Equilibria of Water and Ionic Liquids [emim][PF_6] and [bmim][PF_6]. *Fluid Phase Equilib.* **2002**, *194−197*, 1089–1095.

(23) Krummen, M.; Wasserscheid, P.; Gmehling, J. Measurement of Activity Coefficients at Infinite Dilution in Ionic Liquids Using the Dilutor Technique. *J. Chem. Eng. Data* **2002**, *47*, 1411–1417.

(24) Ye, C.; Shreeve, J. M. Rapid and Accurate Estimation of Densities of Room-Temperature Ionic Liquids and Salts. *J. Phys. Chem. A* **2007**, *111*, 1456–1461.

(25) Blanchard, L. A.; Gu, Z.; Brennecke, J. F. High-Pressure Phase Behavior of Ionic Liquid/CO_2 Systems. *J. Phys. Chem. B* **2001**, *105*, 2437–2444.

(26) Aki, S. N. V. K.; Mellein, B. R.; Saurer, E. M.; Brennecke, J. F. High-Pressure Phase Behavior of Carbon Dioxide with Imidazolium-Based Ionic Liquids. *J. Phys. Chem. B* **2004**, *108*, 20355–20365.

(27) Anthony, J. L.; Anderson, J. L.; Maginn, E. J.; Brennecke, J. F. Anion Effects on Gas Solubility in Ionic Liquids. *J. Phys. Chem. B* **2005**, *109*, 6366–6374.

(28) Jalili, A. H.; Mehdizadeh, A.; Shokouhi, M.; Sakhaeinia, H.; Taghikhani, V. Solubility of CO_2 in 1-(2-hydroxyethyl)-3-methylimidazolium Ionic Liquids with Different Anions. *J. Chem. Thermodyn.* **2010**, *42*, 787–791.

(29) Jacquemin, J.; Husson, P.; Majer, V.; Costa Gomes, M. F. Low-Pressure Solubilities and Thermodynamics of Solvation of Eight Gases in 1-Butyl-3- methylimidazolium Hexafluorophosphate. *Fluid Phase Equilib.* **2006**, *240*, 87–95.

(30) Kumelan, J.; Pérez-Salado Kamps, Á.; Tuma, D.; Yokozeki, A.; Shiflett, M. B.; Maurer, G. Solubility of Tetrafluoromethane in the Ionic Liquid [hmim][Tf_2N]. *J. Phys. Chem. B* **2008**, *112*, 3040–3047.

(31) Seddon, K. R.; Stark, A.; Torres, M.-J. Viscosity and Density of 1-Alkyl-3-methylimidazolium Ionic Liquids. *ACS Symp. Ser.* **2002**, *819*, 34–39.

Received for review July 31, 2010. Accepted October 12, 2010. We are thankful to the research council of the Research Institute of Petroleum Industry (RIPI) and also to the Research and Development of the National Iranian Oil Company (NIOC) for their support of this work.

JE100794K